Int. J. Solids Structures, 1976, Vol. 12, pp. 809–825. Pergamon Press. Printed in Great Britain

THE ANALYSIS OF CYCLICALLY LOADED CREEPING STRUCTURES FOR SHORT CYCLE TIMES

A. R. S. PONTER
Department of Engineering, University of Leicester, Leicester LE1 7RH, England

(*Received* 24 *October* 1975)

Abstract—In a recent paper [1] it was shown that the evaluation of certain bounding solutions for a structure subjected to cyclic loading was equivalent to assuming that the cycle time Δt was short compared with a stress redistribution time. Comparisons between values which are likely to occur in creep design situations indicated that Δt may often be assumed to be small and the bounding solution may be expected to closely approximate the actual stress history. In this paper the solution for the limiting case when $\Delta t \to 0$ is evaluated for a class of constitutive relationships which may be expressed in terms of a finite number of state variables. Strain-hardening viscous, visco-elastic and Bailey–Orowan equations are discussed and particular solutions for which the residual stresses remain constant in time are derived. The solution for a non-linear visco-elastic model indicates that, for the stationary cyclic state, the constitutive equation need only predict the creep strain over a discrete number of cycles and need not predict the strains during a cycle. This observation should considerably simplify creep analysis.

The solution of a simple example demonstrates the similarity between the predicting of the various constitutive relationships for isothermal problems. In fact they provide virtually identical solutions when expressed in terms of reference stress histories. The finite element solution of a plate containing a hole and subjected to variable edge loading is also presented for a viscous material. The solutions show behaviour which is similar to that of the two bar structure.

1. INTRODUCTION

In recent papers [1, 2], the following problem was considered. A body of volume V is subjected to a quasi-static loading history $P_i(t)$ and temperature history $\theta(t)$ which remains cyclic with period Δt. The material suffers both elastic strain $\underline{e}$ and time-hardening creep strains $\underline{v}$. Hence

$$\underline{\epsilon} = \underline{e} + \underline{v} + \underline{\Delta} \tag{1}$$

$$\underline{e} = \mathbf{C}\underline{\sigma} \tag{2}$$

$$\dot{\underline{v}}(\underline{\sigma}) = k\frac{\partial}{\partial \underline{\sigma}}\left\{\frac{\phi^{n+1}}{n+1}\right\} \tag{3}$$

where C denotes a tensor of elastic constants, k a material constant and ϕ a homogeneous function of degree one in the components of stress $\underline{\sigma}$. The thermal expansion strains are given by $\underline{\Delta}$. Although $\underline{\sigma}$ and $\underline{\epsilon}$ were interpreted as the stress and strain tensors within a continuum, they may equally well be understood as generalized stresses and strains within a structure.

At time $t = 0$, the body may possess a residual stress field $\underline{\rho}(0)$, but for large times the stress history approaches a cyclic state, independent of this initial state when $\underline{\sigma}(t) = \underline{\sigma}(t + \Delta t)$. The analysis of Ref. [1] was concerned with the behaviour in this cyclic state. The energy dissipated per cycle is given by

$$\int_V \int_0^{\Delta t} \dot{D}^c \, \mathrm{d}t \, \mathrm{d}V = \int_V \int_0^{\Delta t} k\phi^{n+1}(\underline{\sigma}(t)) \, \mathrm{d}t \, \mathrm{d}V \tag{4}$$

and this quantity may be bounded from above and below by the dissipations associated with two possible equilibrium stress histories:

$$\int_V \int_0^{\Delta t} \dot{D}^c(\underline{\sigma}^s) \, \mathrm{d}t \, \mathrm{d}V \leq \int_V \int_0^{\Delta t} \dot{D}^c(\underline{\sigma}) \, \mathrm{d}t \, \mathrm{d}V \leq \int_V \int_0^{\Delta t} \dot{D}^c(\underline{\sigma}^*) \, \mathrm{d}t \, \mathrm{d}V. \tag{5}$$

The lower bound history $\underline{\sigma}^s$ arises when we assume $\underline{e} = \underline{\Delta} = 0$, and corresponds to the purely

viscous behaviour. The upper bound history $\underline{\sigma}^*$ is given by

$$\underline{\sigma}^*(t) = \hat{\underline{\sigma}} + \bar{\underline{\rho}} \tag{6}$$

where $\hat{\underline{\sigma}}$ denotes the purely elastic response ($\dot{\underline{v}} = 0$) and $\bar{\underline{\rho}}$ denotes a constant residual stress field, i.e. any equilibrium stress field in equilibrium with zero applied loads. The optimal upper bound is found from the condition that the accumulated creep strain corresponding to $\underline{\sigma}^*$

$$\Delta \underline{v} = \int_0^{\Delta t} \dot{\underline{v}}(\underline{\sigma}^*)\, \mathrm{d}t \tag{7}$$

shall be compatible, where $\dot{\underline{v}}$ is given by (3).

An interpretation of this upper bound was described in [1]. The problem is characterized by two distinct time scales, the cycle time Δt, and a parameter which describes the rate at which creep is taking place. This parameter has no unique definition but may be taken as the time for which the steady state creep strain equals the elastic strain at either an average or "representative" stress, or a maximum stress in the cyclic state. Clearly this time scale depends upon both the material characteristics and stresses which occur in the body, and has been employed as a means of characterizing the stress redistribution time for a body under constant load [2, 3].

If we assume that the cycle time is small compared with this characteristic time then, effectively, during a cycle the variation of stress is governed by elastic properties and the residual stress remains constant, providing a stress history of the form of eqn (6). Consideration of typical time scales which occur in design problems indicates that Δt is small when the lifetime of the structure is measured in years, and the cycle time in hours. Williams and Leckie [4] have carried out numerical solutions for a simple two bar structure and find, for parameters which are relevant to design situations, the stress history rapidly assumes a close approximation to the upper bound history.

The advantages of this bounding analysis are evident. The problem reduces to the computation of a residual stress field $\bar{\underline{\rho}}$ and the usual step by step analysis of cyclic loading, both thermal and mechanical, becomes unnecessary. A few simple examples have been presented by Ponter and Williams [5] and Ponter and Leckie [6], for the constitutive relationship eqns (1)–(3). Point displacement bounds have been discussed by Ponter [7].

The principal conclusion we may draw from these considerations is that, in many applications, the cycle time may be considered small compared with characteristic material times. In this paper we investigate the solution which arises when $\Delta t \to 0$ for the general constitutive relationships

where

$$\dot{\underline{\epsilon}} = \dot{\underline{e}} + \dot{\underline{v}} + \dot{\underline{\Delta}} \tag{8}$$

$$\dot{\underline{v}} = \underline{f}(\underline{\sigma}, \underline{s}) \tag{9}$$

$$\dot{\underline{s}} = \underline{g}(\underline{\sigma}, \underline{s}) \tag{10}$$

where $\underline{f}$ and $\underline{g}$ are arbitrary functions of the instantaneous stress state $\underline{\sigma}$ and a vector (or possibly tensor) of state variables $\underline{s}$. In the ensuing analysis it is not necessary to specify these relationships more closely, excepting that we assume that both $\underline{f}$ and $\underline{g}$ are continuous in their arguments. Special cases of these equations are given by eqn (3) where $\underline{s} = 0$ and strain-hardening where $\underline{s} = \underline{v}$ and $\underline{f} = \underline{g}$. Further examples are provided by constitutive relations derived from non-linear rheological models and the Bailey–Orowan model [9, 10]. Minimum principles are then derived from the rate problem arising from the rapid cycling solution.

In the final section a simple example involving variable load and constant temperature is presented which demonstrates that the stress histories generated for the various constitutive relationships are very similar, and that the average displacement rates may be predicted by a uniquely defined reference stress history. For the Bailey–Orowan model the solutions are particularly simple to generate and provide the most straightforward indication of the reference stress history, and may, therefore, be preferable in practice. This result is essentially the same as

that reported by Williams and Leckie[4]. A further example of a stress concentration at a hole exhibits similar behaviour.

However, all the material models discussed here predict continued isotropy of material properties with deformation, and it would seem appropriate to include an equivalent effect to the Bauschinger effect for situations where the stress reverses in sign during a cycle.

2. THE SOLUTION WHEN $\Delta t \to 0$

Consider a body subject to cyclic loading and temperature history. We define by $\hat{\underline{\sigma}}$ the elastic solution to the problem (i.e. $\underline{v} = 0$). The elastic strains

$$\hat{\underline{\varepsilon}} = \mathbf{C}\hat{\underline{\sigma}}$$

are such that $\hat{\underline{\varepsilon}} = \hat{\underline{e}} + \underline{\Delta}$ are compatible, which gives rise to displacements compatible with any imposed surface displacements.

Consider a cycle

$$t_0 \leqslant t \leqslant t_0 + \Delta t.$$

At any instant the stress distribution may be described as

$$\underline{\sigma}(t) = \hat{\underline{\sigma}}(t) + \underline{\rho}(t)$$

where $\underline{\rho}(t)$ is the instantaneous residual stress field.

The governing variables are now transformed to a time variable τ which remains independent of Δt,

$$t = t_0 + \tau \Delta t, \quad 0 \leqslant \tau \leqslant 1$$

and the constitutive relationships (8) to (10) become

$$\mathring{\underline{\varepsilon}} = \mathring{\underline{e}} + \mathring{\underline{v}} + \mathring{\underline{\Delta}} \tag{11}$$

$$\mathring{\underline{e}} = \mathbf{C}\mathring{\underline{\sigma}} \tag{12}$$

$$\mathring{\underline{v}} = \Delta t \underline{f}(\underline{\sigma}(t_0 + \tau \Delta t),\ \underline{s}(t_0 + \tau \Delta t)) \tag{13}$$

$$\mathring{\underline{s}} = \Delta t \underline{g}(\underline{\sigma}, \underline{s}) \tag{14}$$

where

$$\mathring{\underline{\varepsilon}} = \frac{\mathrm{d}}{\mathrm{d}\tau}(\underline{\varepsilon}) \text{ etc.}$$

To evaluate the changes over an entire cycle we define quantities $\bar{\underline{\varepsilon}}, \bar{\underline{e}}, \bar{\underline{s}}, \bar{\underline{\sigma}}$ which coincide with $\underline{\varepsilon}, \underline{e}, \underline{s}$ and $\underline{\sigma}$ at t_0 and $t_0 + \Delta t$ but which vary linearly with time within $0 < \tau < 1$.

The average strain rate is then defined by

$$\begin{aligned}\dot{\bar{\varepsilon}} &= (\bar{\underline{\varepsilon}}(t_0 + \Delta t) - \bar{\underline{\varepsilon}}(t_0))/\Delta t = (\underline{\varepsilon}(t_0 + \Delta t) - \epsilon(t_0))/\Delta t \\ &= \mathbf{C}(\underline{\rho}(t_0 + \Delta t) - \underline{\rho}(t_0))/\Delta t + \dot{\bar{v}},\end{aligned}$$

$$\dot{\bar{v}} = \int_0^1 \underline{f}(\underline{\sigma}, \underline{s})\, \mathrm{d}\tau, \tag{15}$$

as $\quad \hat{\underline{\sigma}}(t_0 + \Delta t) = \hat{\sigma}(t_0).$

Similarly

$$\dot{\bar{s}} = \frac{\underline{s}(t_0 + \Delta t) - \underline{s}(t_0)}{\Delta t} = \int_0^1 \underline{g}(\underline{\sigma}, \underline{s})\, \mathrm{d}\tau. \tag{16}$$

The eqns (11) to (14) provide the behaviour within a cycle whereas eqns (15) and (16) provide the behaviour over a cycle.

In the limit as $\Delta t \to 0$ eqns (13) and (14) yield that $\dot{\underline{v}} = 0$ and $\dot{\underline{s}} = 0$, and hence $\dot{\underline{q}} = \dot{\underline{\sigma}}$. As the elastic solution depends only upon τ then

$$\underline{\sigma}(t_0, \tau) = \hat{\underline{\sigma}}(\tau) + \underline{\rho}(t_0) \tag{17}$$

and

$$\underline{s}(t_0, \tau) = \underline{s}(t_0). \tag{18}$$

With these substitutions the rate equations for the average rates, eqns (15) and (16) become

$$\dot{\bar{\epsilon}} = \mathbf{C}\dot{\underline{\rho}} + \dot{\bar{v}} \tag{19}$$

where

$$\dot{\bar{v}} = \int_0^1 \underline{f}(\hat{\underline{\sigma}}(\tau) + \underline{\rho}(t_0), \underline{s}(t_0))\, \mathrm{d}\tau \tag{20}$$

and

$$\dot{\underline{s}} = \int_0^1 \underline{g}(\hat{\underline{\sigma}}(\tau) + \underline{\rho}(t_0), \underline{s}(t_0))\, \mathrm{d}\tau. \tag{21}$$

As both ρ and s are independent of τ then we need not distinguish between $\tilde{\rho}$ and ρ, $\tilde{s}$ and s.

These equations are supplemented by equilibrium equations for $\underline{\rho}$:

$$\begin{aligned} \rho_{ij,j} &= 0 \quad \text{in } V, \\ \rho_{ij} n_i &= 0 \quad \text{on } S_T, \end{aligned} \tag{22}$$

where n_i denotes an outward normal to S, and the compatibility of $\dot{\underline{\epsilon}}$:

$$\dot{\epsilon}_{ij} = \frac{1}{2}\left(\frac{\partial \dot{\tilde{u}}_i}{\partial x_j} + \frac{\partial \dot{\tilde{u}}_j}{\partial x_i}\right), \tag{23}$$

where $\tilde{u}_i$ denotes compatible displacement rates. Hence eqns (19) to (23) provide a rate boundary value problem at any instant t_0 for $\dot{\bar{\epsilon}}$ and $\dot{\underline{\rho}}$.

The uniqueness of these rates may easily be proven from the positive definiteness of the complementary strain energy density

$$\bar{U}(\sigma_{ij}) = \frac{1}{2} C_{ijkl}\sigma_{ij}\sigma_{kl} \geqslant 0 \tag{24}$$

where equality occurs only when $\sigma_{ij} = 0$. Suppose that two solutions $\dot{\underline{\rho}}^1$ and $\dot{\underline{\rho}}^2$ with associated $\dot{\bar{\epsilon}}^1$ and $\dot{\bar{\epsilon}}^2$ exist at time t_0. By the principle of virtual work

$$A = \int_V (\dot{\bar{\epsilon}}^1 - \dot{\bar{\epsilon}}^2)(\dot{\underline{\rho}}^1 - \dot{\underline{\rho}}^2)\, \mathrm{d}V = 0 \tag{25a}$$

But from (19)

$$A = \int_V \mathbf{C}(\dot{\underline{\rho}}^1 - \dot{\underline{\rho}}^2)(\dot{\underline{\rho}}^1 - \dot{\underline{\rho}}^2)\, \mathrm{d}V = \int_V 2\bar{U}(\dot{\underline{\rho}}^1 - \dot{\underline{\rho}}^2)\, \mathrm{d}V \geqslant 0 \tag{25b}$$

where equality holds only when $\dot{\underline{\rho}}^1 = \dot{\underline{\rho}}^2$ which must hold for consistency between (25a) and (25b). Hence the uniqueness of $\dot{\underline{\rho}}$ is proven.

In the following section three particular cases are considered and steady state solutions are sought for which $\dot{\underline{\rho}} = 0$.

4. NON-LINEAR VISCOUS MATERIAL

To provide continuity with previous work, we first consider the Norton viscous relationship,

$$\dot{v}_{ij}(\sigma_{kl}) = k\frac{\partial}{\partial \sigma_{ij}}\left\{\frac{\phi^{n+1}(\sigma_{kl})}{n+1}\right\} \tag{26}$$

where k denotes a function of temperature and ϕ denotes a homogeneous function of degree one. In Ref. [1] a slightly more general relationship was considered where, in the notation of this paper, $k = k(t)$, but no generality is lost by assuming k remains constant in time. No state variables appear in this relationship and hence

$$\dot{\underline{\varepsilon}} = \mathbf{C}\dot{\underline{\rho}} + \int_0^1 \dot{\underline{v}}(\hat{\underline{\sigma}}(\tau) + \underline{\rho}(t_0))\,\mathrm{d}\tau. \tag{27}$$

For the cyclic state, which occurs as $t_0 \to \infty$ then $\dot{\underline{\rho}} \to 0$ and (27) and (23) become the condition for the optimal upper bound described in [1], thereby recovering the result that the optimal bound of (5) corresponds to the solution when $\Delta t \to 0$. The complete eqn (27) when $\dot{\underline{\rho}} \neq 0$ provides a transient problem for some assumed initial state $\underline{\rho}(0)$.

5. STRAIN-HARDENING MATERIAL

Primary creep may be described by the time-hardening equation

$$v_{ij} = B\frac{\partial}{\partial \sigma_{ij}}\left\{\frac{\phi^{n+1}}{n+1}\right\}t^m \tag{28}$$

where B denotes a function of temperature and m a time index which is often given the value $m = 1/3$. The creep rate becomes

$$\dot{v}_{ij} = B\frac{\partial}{\partial \sigma_{ij}}\left\{\frac{\phi^{n+1}}{n+1}\right\}mt^{m-1}. \tag{29}$$

If it is assumed that the state of the material is described by the accumulated creep strain v_{ij}, then a strain hardening relationship is formed by eliminating t between eqns (28) and (29) to yield

$$\dot{v}_{ij} = mB^{1/m}\phi^{n/m}(v_{kl}v_{kl}/n_{rs}n_{rs})^{(m-1)/2m}n_{ij} \tag{30}$$

where $n_{ij} = \partial\phi/\partial\sigma_{ij}$ is homogeneous of degree zero in σ_{kl}.

In terms of the general eqns (9) and (10) $\underline{f} = \underline{g}$ and $\underline{v} = \underline{s}$. Hence the equation for rapid cycling is given by

$$\dot{\underline{\varepsilon}} = \mathbf{C}\dot{\rho} + \dot{\underline{v}} \tag{31}$$

where

$$\dot{v}_{ij} = m(v_{kl}v_{kl})^{(m-1)/2m}H_{ij} \tag{32}$$

where

$$H_{ij} = \int_0^1 B^{1/m}\phi^{n/m}(\underline{\sigma})n_{ij}/(n_{rs}n_{rs})^{(m-1)/2m}\,\mathrm{d}\tau \tag{33}$$

and

$$\underline{\sigma} = \hat{\underline{\sigma}}(\tau) + \underline{\rho}(t_0).$$

It is worth noting that the existence of a cyclic solution for finite cycle times has never been proven for this constitutive relationship. We find however that such a solution does exist for $\Delta t \to 0$. Setting $\dot{\underline{\rho}} = 0$ we search for a solution of eqn (32) of the form

$$\dot{\underline{\varepsilon}} = \dot{\underline{v}} = \underline{v}^* t^m$$

where $\underline{v}^*$ denotes a time independent compatible strain field. Such a solution would correspond to some, yet to be determined, initial residual stress field which subsequently remains constant in time.

Substituting into eqn (32) and cancelling mt^{m-1} from both sides yields

$$\underline{v}^*_{ij} = (v^*_{kl}v^*_{kl})^{(m-1)/2m}H_{ij}. \tag{34}$$

Hence

$$\sqrt{(v_{ij}^* v_{ij}^*)} = (v_{kl}^* v_{kl}^*)^{(m-1)/2m} \sqrt{(H_{ij} H_{ij})}. \tag{35}$$

Eliminating v_{ij}^* from the right hand side of (34) by means of (35) yields

$$v_{ij}^* = (H_{kl} H_{kl})^{(m-1)/2} H_{ij}, \quad \bar{v} = \underline{v}^* t^m \tag{36}$$

where H_{ij} is given by eqn (33). Equation (36) is now supplemented by the equilibrium equation for ρ_{ij} and compatibility of v_{ij}^*. The equation has a resemblance to the expression for $\dot{\epsilon}_{ij}$ for the viscous material. The similarity is shown more clearly when both eqns (27) and (36) are specialized to a uniaxial stress history which would become appropriate in, for example, the analysis of a pin-jointed frame. Setting $n_{11} = 1$ with all other $n_{ij} = 0$ and $\phi = \sigma$ yields,

$$\dot{\bar{\epsilon}} = k \int_0^t (\hat{\sigma} + \bar{\rho})^n \, d\tau \quad \text{viscous}, \tag{37}$$

and

$$v^* = B \left\{ \int_0^t (\hat{\sigma} + \bar{\rho})^{n/m} \, d\tau \right\}^m, \quad \dot{\bar{\epsilon}} = v^* m t^{m-1} \quad \text{strain-hardening}. \tag{38}$$

When $\hat{\sigma}$ = constant, the two relationships are formally identical, if $k = Bmt^{m-1}$.

6. NON-LINEAR VISCO-ELASTICITY

A further class of constitutive relationships have been discussed by Besselling[8], which are, essentially, constitutive relationships derived from visco-elastic models composed of linear springs and non-linear dashpots.

The ability of such models to describe creep behaviour is uncertain as they generally exhibit excessive creep strain recovery, i.e. the recovery of inelastic strain after the removal of stress. They also fail to exhibit creep hesitation, the small creep rate which follows a reduction in stress, which is exhibited in most metals. These models do however describe the so-called anelastic strain, a recoverable primary creep strain which can be pronounced in some metals.

Consider the typical model shown in Fig. 1, a non-linear version of the standard linear solid, much used in linear visco-elasticity theory. We generalize this model to a triaxial state of stress by

$$\sigma_{ij} = \sigma_{ij}^1 + \sigma_{ij}^2 \tag{39}$$

$$\dot{v}_{ij}^1 = G_{ijkl} \dot{\sigma}_{kl}^1 = k_1 \phi^r (\sigma_{kl}^2) \frac{\partial \phi}{\partial \sigma_{ij}^2} \tag{40}$$

and

$$\dot{v}_{ij}^2 = k_2 \phi^n (\sigma_{kl}) \frac{\partial \phi}{2 \sigma_{ij}} \tag{41}$$

$$v_{ij} = v_{ij}^1 + v_{ij}^2. \tag{42}$$

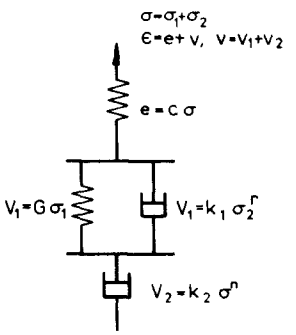

Fig. 1. Uniaxial non-linear visco-elastic model, which forms the basis of constitutive relationships (39) to (42).

Here r and n are creep indices and ϕ denotes, as before, a homogeneous function of degree unity. To transform these equations into the form of eqns (9) and (10) a single internal state variable is identified with σ^1_{ij}, the stress in the spring of the Voight element. Equating $s_{ij} = \sigma^1_{ij}$ eqn (39) to (42) may be written in the form

$$\dot{v}_{ij} = k_1\phi^r(\sigma_{kl} - s_{kl})\left(\frac{\partial\phi}{\partial\sigma_{ij}}\right)_{\sigma-s} + k_2\phi^n(\sigma_{kl})\frac{\partial\phi}{\partial\sigma_{ij}} \tag{43}$$

$$\dot{s}_{ij} = L_{ijrs}k_1\phi^r(\sigma_{kl} - s_{kl})\left(\frac{\partial\phi}{\partial\sigma_{rs}}\right)_{\sigma-s} \tag{44}$$

where L_{ijks} denotes the inverse of G_{ijkl}, i.e.

$$\dot{s}_{ij} = \dot{\sigma}^1_{ij} = L_{ijkl}\dot{v}^1_{kl}. \tag{45}$$

For rapid cyclic loading

$$\dot{s}_{ij} = L_{ijrs}\int_0^1 k_1\phi^r(\hat{\sigma}_{kl} + \rho_{kl} - s_{kl})\frac{\partial\phi}{\partial\sigma_{rs}}\,d\tau.$$

For the cyclic solution $\dot{s}_{ij} = 0$ providing equation for s_{kl} in terms of ρ_{kl}. The average rate is given by

$$\dot{\bar{\epsilon}}_{ij} = C\dot{\rho}_{kl} + G_{ijkl}\dot{s}_{kl} + \int_0^1 k_2\phi^n(\hat{\sigma}_{kl} + \rho_{kl})\frac{\partial\phi}{\partial\sigma_{ij}}\,d\tau. \tag{47}$$

For the cyclic state as both $\dot{\rho}_{kl}$ and $\dot{s}_{kl}$ are zero the resulting expression is identical to the average strain rate provided by the case $k_1 = 0$, i.e. the non-linear Maxwell model without the Voight element. Hence the value of ρ_{kl} and $\dot{\bar{\epsilon}}_{ij}$ are entirely independent of both s_{kl} and the characteristics of the Voight element. In other words, as the average creep rate $\dot{\bar{\epsilon}}_{ij}$ and ρ_{kl} are computed from the accumulation over a cycle, any element of the constitutive relationship which provides no accumulation of strain may be effectively ignored when considering the cyclic behaviour. A constitutive relationship which provided the correct accumulation of strain per cycle for cyclic stress histories is all that is required for the evaluation of the rapid cyclic behaviour.

If it is accepted that a design problem involves rapid cycling, this analysis implies that it is not necessary to develop constitutive relationships which are capable of predicting the strain history within a cycle, but only over a discrete number of cycles. This observation should considerably simplify the search for suitable constitutive relation for creep.

7. THE BAILEY-OROWAN MODEL

Finally we discuss a constitutive equation which includes the effect of thermal recovery, and has been discussed by Ponter and Leckie[9],

$$\dot{v}_{ij} = f(\phi(\sigma_{kl}) - s)\frac{\partial\phi}{\partial\sigma_{ij}} \tag{48a}$$

$$\dot{s} = h(s)f - r(s) \tag{48b}$$

where s denotes an internal state variable, the yield stress and f denotes a function defined by

$$\begin{aligned} f(\phi - s) &> 0 \quad \phi = s \\ f(\phi - s) &= 0 \quad \phi < s. \end{aligned} \tag{49}$$

The functions h and r are given by

$$h(s) = 1/k_1 s^{n-\alpha}, \quad r(s) = k_2 s^{\alpha}.$$

When σ_{ij} is constant, $\phi = s$ and $\dot{s} = 0$ then

$$\dot{v}_{ij} = \frac{r(\phi)}{h(\phi)} \frac{\partial \phi}{\partial \sigma_{ij}} = k \frac{\partial}{\partial \sigma_{ij}} \left\{ \frac{\phi^{n+1}}{n+1} \right\}, \quad k = k_1 k_2 \tag{50}$$

and stationary state creep is recovered. The quantities k_1 and k_2 are both functions of the instantaneous temperature, although for all practical purposes k_1 can be considered as independent of temperature.

The average creep rate for rapid cycling is given by

$$\dot{\bar{v}} = \int_0^1 f(\phi - s) \frac{\partial \phi}{\partial \sigma_{ij}} \, d\tau, \tag{51a}$$

$$\dot{s} = h(s) \int_0^1 f \, d\tau - \bar{r}(s), \quad \sigma_{ij} = \hat{\sigma}_{ij}(\tau) + \rho_{ij}(t_0), \quad \bar{r}(s) = \int_0^1 k_2 \, d\tau s^{\alpha}, \tag{51b}$$

for the cyclic state when $\dot{s} = 0$, then, as $\phi \leqslant s$

$$s = \max \phi(\hat{\sigma}_{ij}(\tau) + \rho_{ij}(t_0)).$$

If we denote the instant when the maximum occurs by τ_0 with corresponding ϕ_0, then

$$\dot{\bar{v}}_{ij} = \frac{\bar{r}(\phi_0)}{h(\phi_0)} \frac{\partial \phi_0}{\partial \sigma_{ij}} \tag{52}$$

by eliminating f from (51a) and (51b). Hence the average creep rate is that of the steady state creep rate of the stress in the history $\hat{\sigma}_{ij}(\tau) + \rho_{ij}(t_0)$ which maximizes ϕ when the effects of temperature are averaged over a cycle. This result was given in a different way in [10].

The eqn (52) provides the average creep rate when a distinct continuous time interval (or instant) occurs when ϕ_0 remains constant. There remains the possibility that ϕ achieves equal maximum values at two or more distinct instants τ_0, τ_1, τ_2 etc. Consider the case where two times occur, τ_0 and τ_1 where ϕ achieves equal values $\phi_0 = \phi_1$ which are greater than at any other time. Equation (51a) and (51b) now yield

$$\alpha_0 + \alpha_1 = \frac{h(s)}{r(s)}, \quad s = \phi_0 = \phi_1$$

$$\dot{\bar{v}}_{ij} = \alpha_0 \frac{\partial \phi_0}{\partial \sigma_{ij}} + \alpha_1 \frac{\partial \phi_1}{\partial \sigma_{ij}}$$

where α_0 and α_1 are the contributions to $\int_0^1 f \, d\tau$ at τ_0 and τ_1. Hence

$$\dot{\bar{v}}_{ij} = \left(\frac{\alpha_0}{\alpha_0 + \alpha_1} \right) \frac{h(\phi_0)}{\bar{r}(\phi_0)} \frac{\partial \phi_0}{\partial \sigma_{ij}} + \left(\frac{\alpha_1}{\alpha_0 + \alpha_1} \right) \frac{h(\phi_1)}{\bar{r}(\phi_1)} \frac{\partial \phi_1}{\partial \sigma_{ij}} \tag{53}$$

and $\dot{\bar{v}}_{ij}$ becomes any linearly interpolated value of the stationary state values corresponding to τ_0 and τ_1.

8. MINIMUM PRINCIPLES

Consider a body subject to a rapid cyclic history of loading $P_i(t)$ over part of its surface S_T and surface displacements over S_u the remainder of S. At some time t_0 the current residual stress ρ_{ij} is assumed known. The minimum principles are concerned with the average strain, displacement and residual stress rate at this instant.

The elastic strain energy density $U(\epsilon_{ij})$ is given by

$$U = \frac{1}{2} G_{ijkl} \epsilon_{ij} \epsilon_{kl}, \quad \frac{\partial U}{\partial \epsilon_{ij}} = G_{ijkl} \epsilon_{kl} \tag{54}$$

where G_{ijkl} is the inverse of C_{ijkl}. Both U and $\bar{U}$, defined by (24) are assumed to be convex

$$U(\epsilon_{kl}^1) - U(\epsilon_{kl}^2) - \frac{\partial U}{\partial \epsilon_{ij}^2}(\epsilon_{ij}^1 - \epsilon_{ij}^2) \geq 0 \tag{55}$$

$$\bar{U}(\sigma_{kl}^1) - \bar{U}(\sigma_{kl}^2) - \frac{\partial \bar{U}}{\partial \sigma_{ij}^2}(\sigma_{ij}^1 - \sigma_{ij}^2) \geq 0 \tag{56}$$

At time $t = t_0$, the actual average strain rate is given by $\dot{\bar{\epsilon}}_{ij}$. Consider an arbitrary compatible strain rate field $\dot{\bar{\epsilon}}_{ij}^c$ which gives rise to zero displacement rate on S_u.

Theorem 1: Amongst all compatible strain rate fields $\dot{\bar{\epsilon}}_{ij}^c$, $\dot{\bar{\epsilon}}_{ij}$ minimizes

$$\int_V U(\dot{\bar{\epsilon}}_{ij}^c - \dot{\bar{v}}_{ij})\,\mathrm{d}V.$$

This result follows when $\epsilon_{ij}^1 = \dot{\bar{\epsilon}}_{ij}^c - \dot{\bar{v}}_{ij}$ and $\epsilon_{ij}^2 = \dot{\bar{\epsilon}}_{ij} - \dot{\bar{v}}_{ij}$ are substituted into (55). On noting (19) then (55), integrated over the volume V, becomes

$$\int_V U(\dot{\bar{\epsilon}}_{ij}^c - \dot{\bar{v}}_{ij})\,\mathrm{d}V - \int_V U(\dot{\bar{\epsilon}}_{ij} - \dot{\bar{v}}_{ij})\,\mathrm{d}V - \int_V \dot{\rho}_{ij}(\dot{\bar{\epsilon}}_{ij}^c - \dot{\bar{\epsilon}}_{ij})\,\mathrm{d}V \geq 0.$$

By the principle of virtual work

$$\int_V \dot{\rho}_{ij}(\dot{\bar{\epsilon}}_{ij}^c - \dot{\bar{\epsilon}}_{ij})\,\mathrm{d}V = 0,$$

and the result then follows.

Theorem 2: Amongst all equilibrium stress rate fields $\dot{\rho}_{ij}^*$ the actual field $\dot{\rho}_{ij}$ provides the absolute minimum of

$$\int_V \{\bar{U}(\dot{\rho}_{ij}^*) + \dot{\rho}_{ij}^* \dot{\bar{v}}_{ij}\}\,\mathrm{d}V$$

where $\dot{\bar{v}}_{ij}$ is given by eqn (20).

The result follows from the convexity condition (56) with $\sigma_{ij}^1 = \dot{\rho}_{ij}^*$ and $\sigma_{ij}^2 = \dot{\rho}_{ij}$, the actual residual stress rate field. On noting (19) the convexity condition (56) becomes, when integrated over the volume,

$$\int_V \{U(\dot{\rho}_{ij}^*) + \dot{\rho}_{ij}^* \dot{\bar{v}}_{ij}\}\,\mathrm{d}V - \int_V \{\bar{U}(\dot{\rho}_{ij}) + \rho_{ij}\dot{\bar{v}}_{ij}\}\,\mathrm{d}V - \int_V \dot{\bar{\epsilon}}_{ij}(\dot{\rho}_{ij}^* - \dot{\rho}_{ij})\,\mathrm{d}V \geq 0.$$

By the principle of virtual work,

$$\int_V \dot{\bar{\epsilon}}_{ij}(\dot{\rho}_{ij}^* - \dot{\rho}_{ij})\,\mathrm{d}V = 0$$

and the result follows.

Theorem 1 provides the basis of a finite element method which will be discussed in [11].

9. AN EXAMPLE

To indicate the type of information which may be gained from the analysis described above, a simple two bar structure is analysed in this section, and a result due to Williams and Leckie [4] is reproduced.

Consider the structure shown in Fig. 2. Two bars of equal cross-sectional area A and length ℓ and 4ℓ are restrained, under the action of an axial load P, to suffer equal axial extension. The elastic solution is given by

$$\hat{\sigma}_1 = 0.8P/A, \quad \hat{\sigma}_2 = 0.2P/A \tag{57}$$

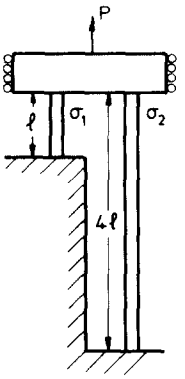

Fig. 2.

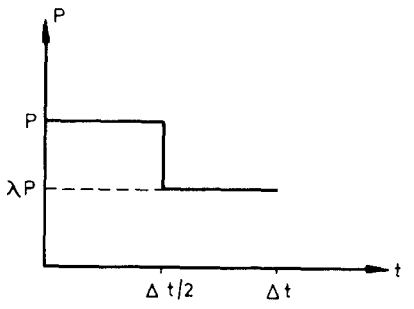

Fig. 3.

and the structure therefore has an elastic stress concentration factor of 4. A residual stress field is given by

$$\bar{\rho}_1 = -R/A, \quad \bar{\rho}_2 = +R/A. \tag{58}$$

The load P follows a cyclic history of the form shown in Fig. 3, where the load parameter λ varies through the range

$$-1 < \lambda < 1.$$

The extreme cases corresponding to constant load ($\lambda = 1$) and equal times at $\pm P$ ($\lambda = -1$). The rapid cycling solution was generated for both the viscous, strain-hardening and Bailey–Orowan constitutive relationship, for which the average strain rates are given by eqns (37), (38) and either (52) or (53).

Viscous material

The value of R for the rapid cycling solution is given by the compatibility equation

$$\dot{\bar{\epsilon}}_1 = 4\dot{\bar{\epsilon}}_2,$$

i.e.

$$\int_0^1 (\hat{\sigma}_1 + \bar{\rho}_1)^n \, d\tau = 4 \int_0^1 (\hat{\sigma}_2 + \bar{\rho}_2)^n \, d\tau, \tag{59}$$

which, on substitution of (57) and (58) yields on eqn for R/P. Equation (59) was solved numerically by Newton's method. The variation of R/P with λ for $n = 3$, 5 and 7 are shown in Fig. 4. The dashed lines correspond to the value corresponding to $\lambda = 1$, the steady state solution for P constant. It is clear that R/P and hence σ_1 and σ_2 for the maximum load varies very little with λ for $-0.3 < \lambda < 1$, and hence the stress histories are little effected by the value of the smaller load λP. For $-1 < \lambda < 0.3$, R/P closely approximates the value $0.4(1 + \lambda)$, especially for the higher values of n. The reason for this is not hard to find. For negative λ, the stresses in bar 1 oscillate between near equal positive and negative values, i.e.

$$0.8P/A - R/A = -(0.8\lambda P/A - R/A)$$

and hence

$$R/P = 0.4(1 + \lambda). \tag{60}$$

In bar 2 the stress history becomes

$$\left.\begin{aligned} \hat{\sigma}_2 + \bar{\rho}_2 &= 0.2P/A + R/A = (0.6 + 0.4\lambda)P/A, \; 0 < \tau < \tfrac{1}{2} \\ \hat{\sigma}_2 + \bar{\rho}_2 &= 0.2\lambda P/A + R/A = (0.4 + 0.6\lambda)P/A, \; \tfrac{1}{2} < \tau < 1 \end{aligned}\right\}. \tag{61}$$

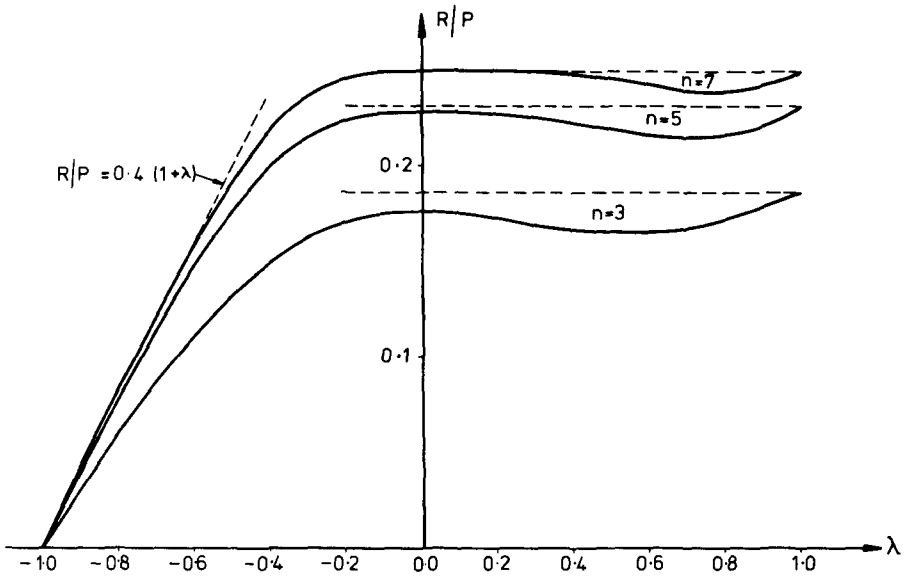

Fig. 4. Variation of residual stress R/P for viscous material.

In Figs. 5–7 the average displacement rate $\dot{\bar{u}}(\lambda)$ is shown normalized with respect to the constant load value $\dot{\bar{u}}(1)$, and is compared with the results of two elementary calculations. The dashed line for $\lambda > 0$ is the displacement rate assuming the steady state solution remains valid throughout the cycle, i.e.

$$\dot{\bar{u}} = \dot{\bar{u}}(1)(1+\lambda^n)/2. \tag{62}$$

This solution gives a good approximation over the range $-0.3 < \lambda < 1$. The second dashed line is the displacement rate evaluated from the stress history (61) and gives a good approximation for $-1 < \lambda < -0.3$ especially for higher values of n.

The calculation (62) is of course equivalent to a reference stress calculation, where the reference stress remains proportional to the applied load. For negative λ this calculation is then superceded by the stress history (61).

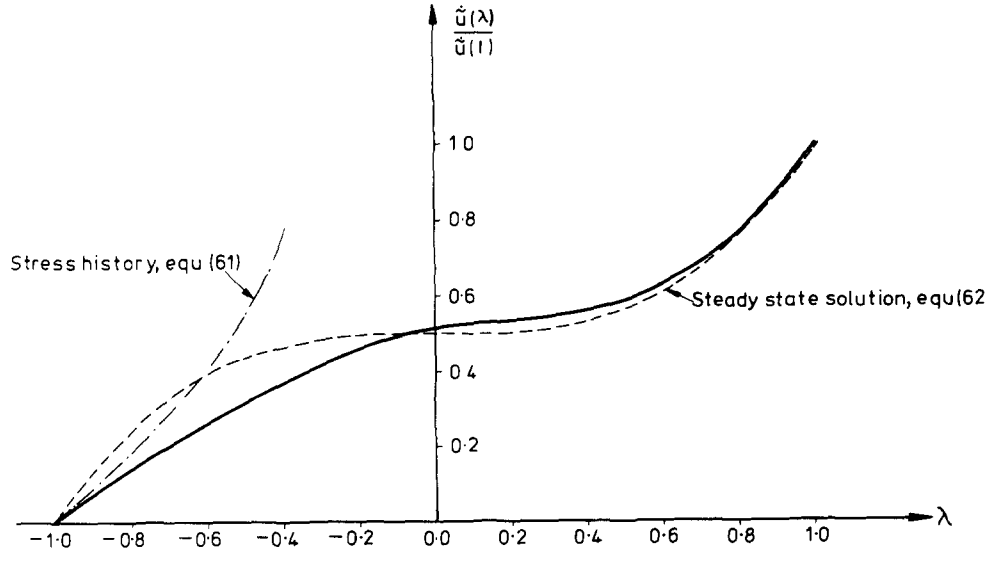

Fig. 5. Variation of average displacement rate for viscous material, $n = 3$.

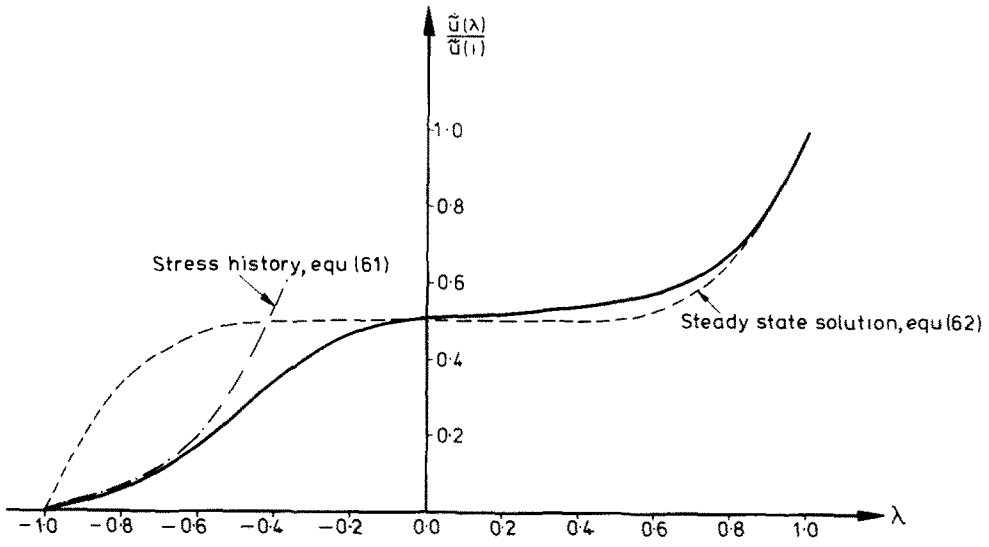

Fig. 6. Variation of average displacement rate for viscous material, $n = 5$.

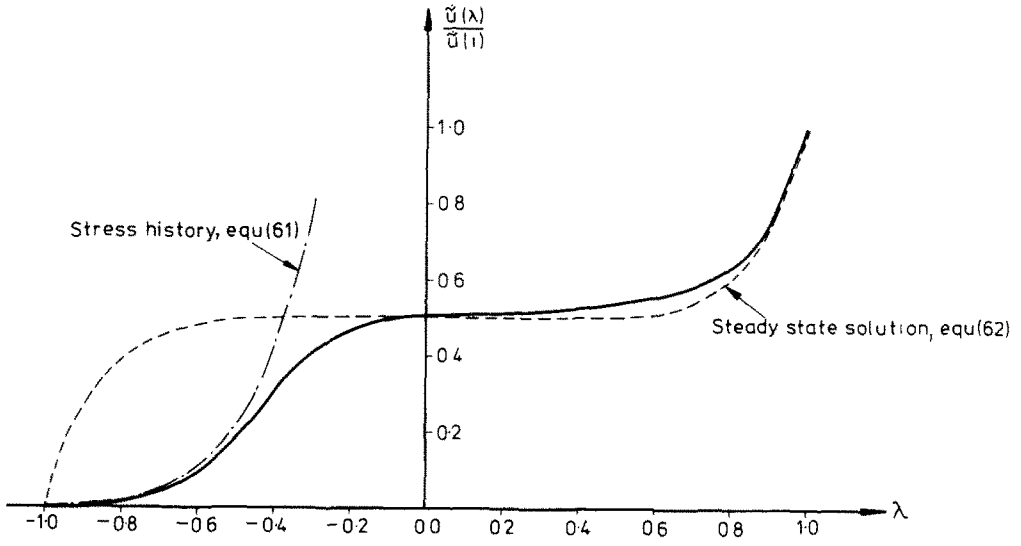

Fig. 7. Variation of average displacement rate for viscous material, $n = 7$.

This result is not surprising, and the correlation with (62) for $\lambda > 1$ has been noted in various ways many times before. The interesting result comes when we compare these solutions with those of strain-hardening, and the Bailey–Orowan model.

Strain-hardening material

The rapid cycling solution requires compatibility of v^* (eqn 38) and hence R/P is given by $v_1^* = 4v_2^*$, i.e.

$$\left\{\int_0^1 (\hat{\sigma}_1 + \bar{\rho}_1)^{n/m}\, d\tau\right\}^m = 4\left\{\int_0^1 (\hat{\sigma}_2 + \bar{\rho}_2)^{n/m}\, d\tau\right\}^m. \tag{63}$$

Equation (63) was solved for R/P with $m = 1/3$ and $n = 3, 5$ and 7. When $\lambda = 1$, the integrands of (63) are constant and hence yield the same equation as (59). The variation of R/P with λ is shown in Fig. 8 and it can be seen immediately that R/P retains a close approximation to the steady state value ($\lambda = 1$) for $-0.3 < \lambda < 1$, and then rapidly becomes close to the value $R/P = 0.4(1 + \lambda)$. Hence the stress histories are very similar to those of the viscous case, with even less deviation

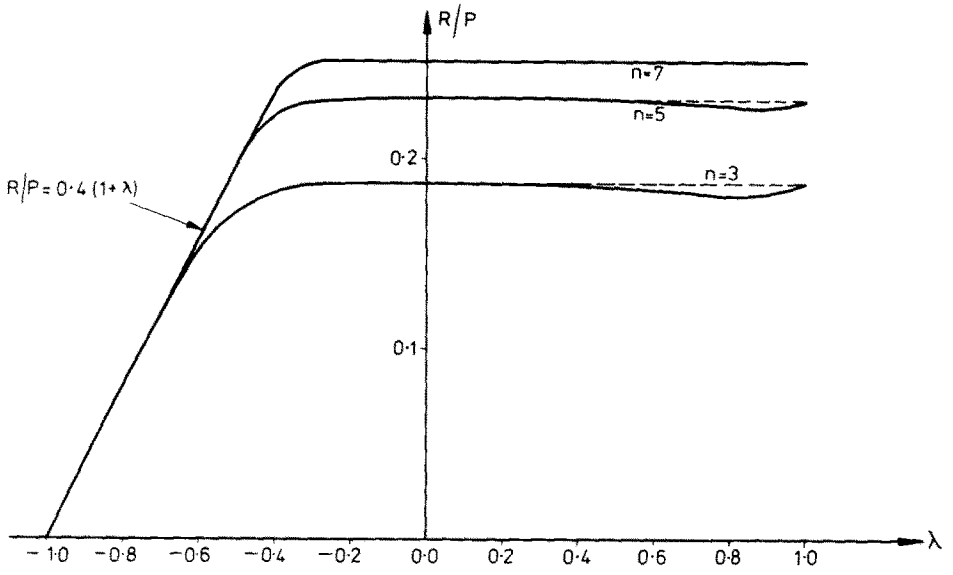

Fig. 8. Variation of residual stress R/P for strain hardening with $m = 1/3$.

from the two simple approximations. The normalized average displacement rate $\dot{\bar{u}}(\lambda)/\dot{\bar{u}}(1)$ is shown in Figs. 9–11 for $n = 3$, 5 and 7, and are compared with two calculations.

If we assume that a reference stress, derivable from the steady state solution remains valid, then the displacement rate must be computed on the assumption that the cycle time is short, and hence be given by eqn (38). Therefore, if a reference stress history follows the applied load, the average displacement rate would be given by

$$\dot{\bar{u}}(\lambda) = \dot{\bar{u}}(1)\left\{\int_0^1 (P(t)/P)^{n/m}\right\}^m = \dot{\bar{u}}(1)\left\{\int_0^1 (1+\lambda^{n/m})/2\right\}^m. \tag{64}$$

This equation appears as a dashed line in Figs. 9–11 and very closely approximates the rapid cycling solution for $-0.3 < \lambda < 1$. For $\lambda < 0.3$, a prediction for the stress history (61) yields

$$\dot{\bar{u}}(\lambda) = \dot{\bar{u}}(1)\left\{\frac{(0.6+0.4\lambda)^{n/m} + (0.4+0.6\lambda)^{n/m}}{2}\right\}^m \tag{65}$$

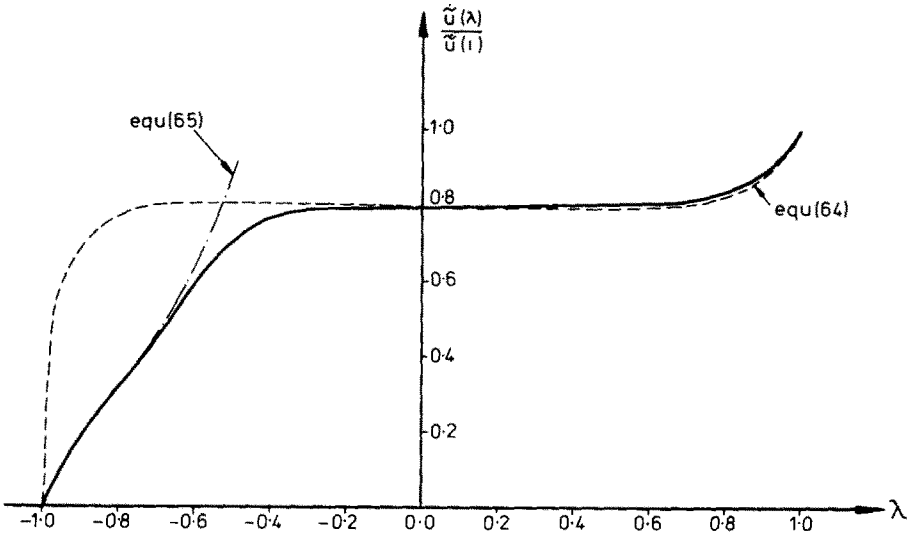

Fig. 9. Variation of average displacement rate, strain hardening, $n = 3$, $m = 1/3$.

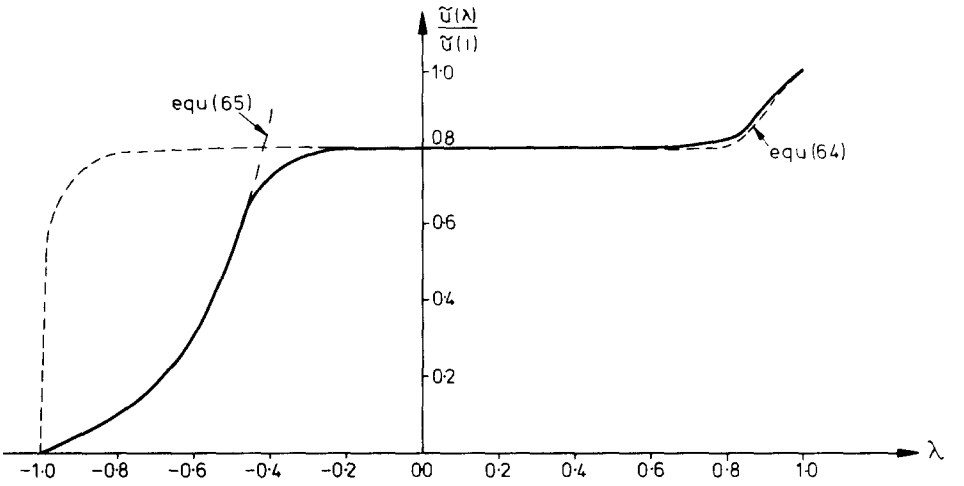

Fig. 10. Variation of average displacement rate, strain hardening, $n = 5, m = 1/3$.

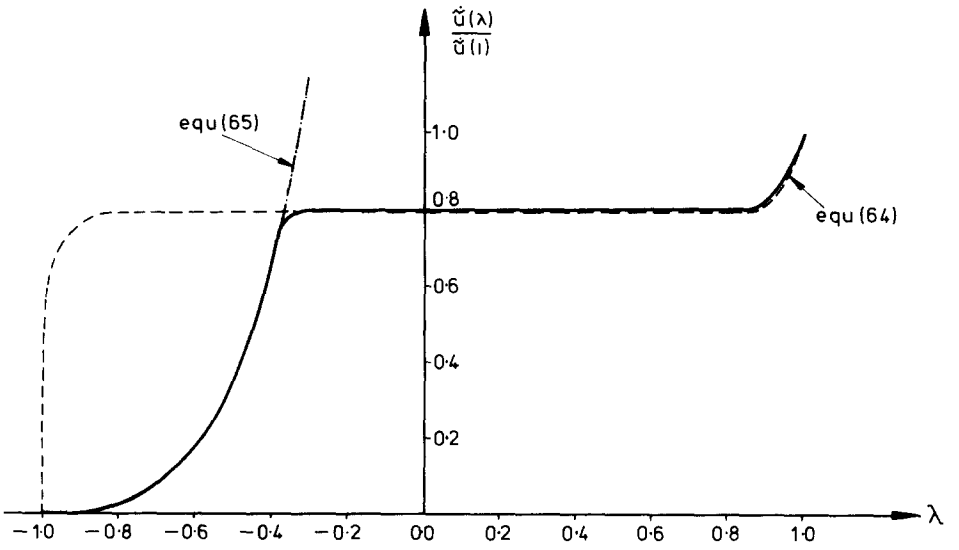

Fig. 11. Variation of average displacement rate, strain hardening $n = 7, m = 1/3$.

and is also shown as a dashed line, and closely approximates the rapid cycling solution for $\lambda < 0.3$.

It is worth noting that over a substantial range of λ, $\dot{\bar{u}}(\lambda)/\dot{\bar{u}}(1)$ remains constant and is independent of n. This value arises in eqn (58) when we assume that $\lambda^{n/m} \ll 1$ and hence

$$\dot{\bar{u}}(\lambda)/\dot{\bar{u}}(1) = 0.5^m = 0.7937, \quad m = 1/3$$

and is equivalent to assuming that all the deformation occurs when $P(t)$ has its maximum value.

The Bailey–Orowan model

The analysis of the rapid-cycling solution for the Bailey–Orowan model is extremely simple. For $\lambda > 1$ the largest stress in both bars may be expected to occur when the applied load is at a maximum, i.e. $0 < \tau < 1/2$. Compatibility of the average creep strain rates, which equals the strain rate at the maximum stress, then provides the solution that the stresses during $0 < \tau < 1/2$ are identical to the viscous solution for constant load. Further the average displacement rate $\dot{\bar{u}}(\lambda) = \dot{\bar{u}}(1)$, the value corresponding to constant applied load P. Clearly the reference stress history generated by the stationary state solution will give the exact answer in this case, assuming rapid cycling.

This solution remains valid until the stress in tension and compression are of equal value in bar 1, i.e.

$$R/P = 0.4(1+\lambda)$$

and the average strain rate in bar 1 becomes indeterminate (eqn 53). The average displacement rate is now governed by the stress history in bar 2 which has the form (61) exactly. Hence the reference stress histories which provided good approximate values of $\dot{\bar{u}}(\lambda)$ for the viscous and strain-hardening models yield the exact values in this case.

The variations of R/P and $\dot{\bar{u}}(\lambda)/\dot{\bar{u}}(1)$ are shown in Figs. 12 and 13 for $n = 3$, 5 and 7. For $\lambda = -1$ there is an indeterminacy of $\dot{\bar{u}}(\lambda)$ as stress in both bar 1 and bar 2 oscillate between equal positive and negative values. Dashed lines, corresponding to the predictions of reference stress histories are excluded as they are identical to the exact values.

It is interesting to compare Figs. 4, 8 and 12, the variation of R/P for the three material models. The differences are really quite small, the strain hardening values (Fig. 8) lying between those of the other two models.

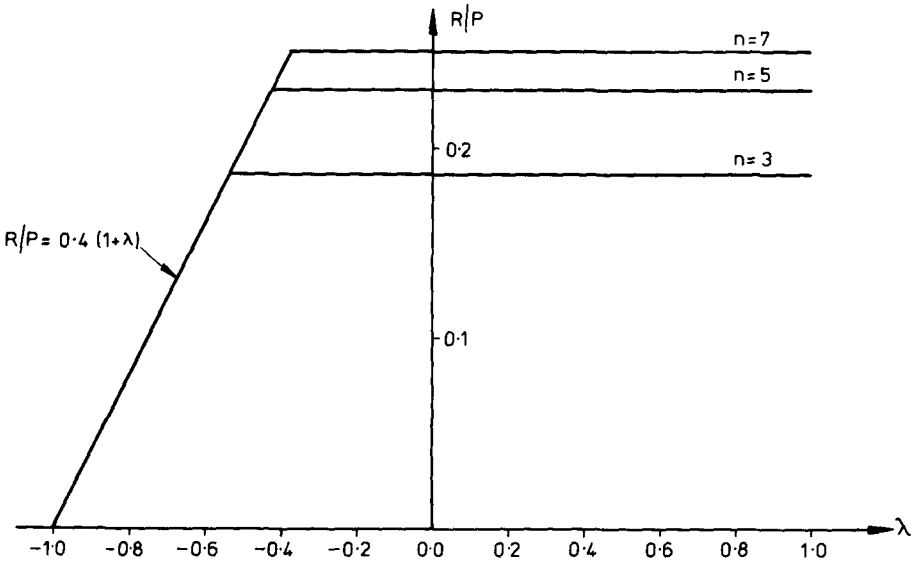

Fig. 12. Variation of residual stress R/P for Bailey–Orowan model.

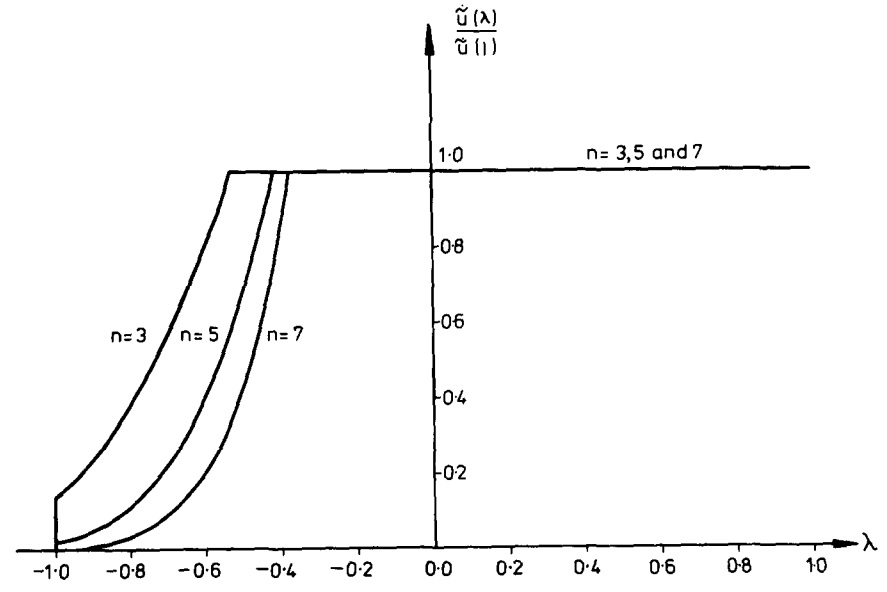

Fig. 13. Variation of average displacement rate, Bailey–Orowan model.

Comparison of the graphs for $\dot{u}(\lambda)/\dot{u}(1)$, Figs. 5–7, 9–11 and Fig. 13 show a similar graduation from viscous behaviour to the Bailey–Orowan model, with strain hardening lying between. In all cases the reference stress predictions provide good approximations to the solutions, given the exact answer for the Bailey–Orowan model. This result is essentially the same as the observations of Williams and Leckie[4]. Further for $\lambda > 0$ there exists at most a factor of 2 differences in $\dot{u}(\lambda)$ for all the models and for $\lambda < 0$ a factor of about 3 for equal n values. Experimental creep rates often suffer from variations which are greater than these factors, indicating that the model adopted is relatively unimportant. On balance, the Bailey–Orowan model appears to be preferable, as the solutions are very simple, although the situation may not remain when more complex structures are considered. Further, very simple displacement bounds exist for the model[10] which indicate that, for certain classes of loading the rapid cycling solution provides an upper bound to the displacements for longer cycle times.

The fact that the three models produce such similar solutions may however lull one into a sense of false security. They, and all isotropic models, imply a continued state of isotropy with developing creep strain. An effect corresponding to the Bauschinger effect in plasticity must exist in creep, and such an effect is not included in any of the models.

Finite element solution

The development of a finite element method from the strain minimum principle of Section 8 is described elsewhere[11]. Here the solution of a classic stress concentration problem is described, the stress distribution around a hole in a plate subject to uniform tension, as shown in Fig. 14. The load history is that of Fig. 3, excepting that P is now interpreted as the uniform stress state away from the hole.

Details of the solution method and finite element mesh are given in [11] together with a wide range of solutions. Here we discuss the viscous solutions. The maximum stress, which occurs at A in Fig. 14, is given in Table 1 together with the minimum stress at that point for $n = 3$ and 5. The general mode of behaviour of the two bar structure is clearly seen. For $\lambda = 0.5$ and 0 the maximum stress lies very close to the value for $\lambda = 1$ when P remains constant. For $\lambda = -0.5$, the stress oscillates between near equal positive and negative values of σ_{xx}. For $\lambda = -1$, of course the residual stress field is zero and the stresses are given by the elastic solution, which has a

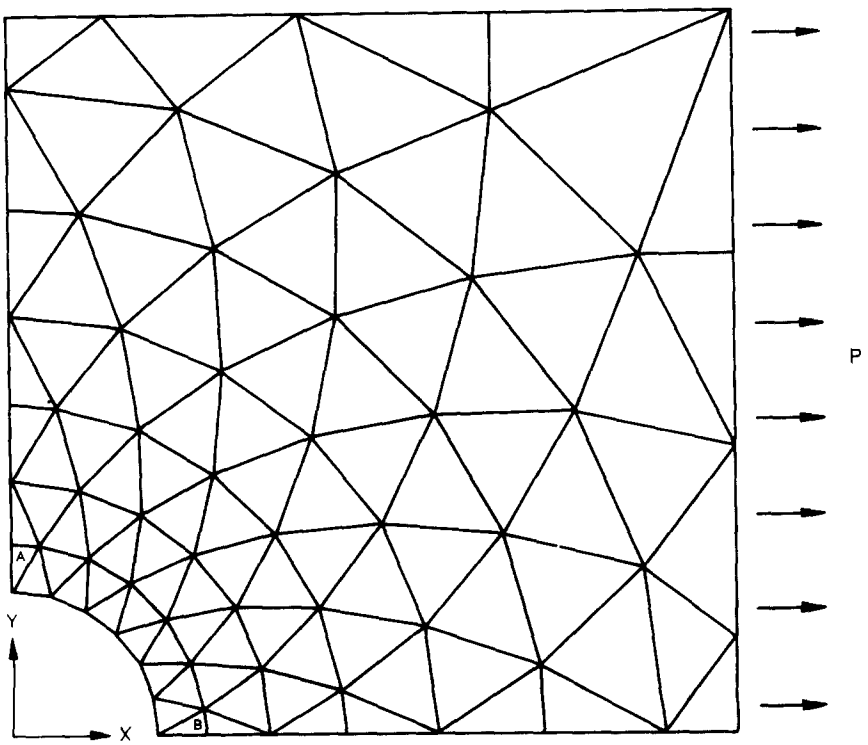

Fig. 14. Finite element mesh for plate subjected to uniform loading.

Table 1. Maximum and minimum values of σ_{xx}/P in element. A—Finite element solution of plate with hole

λ		-1	$-\frac{1}{2}$	0	$\frac{1}{2}$	1
$n=3$	max.	2·98	2·47	2·06	2·06	2·09
	min	−2·98	−2·04	−0·94	0·56	2·09
$n=5$	max.	2·98	2·31	1 80	1·76	1·74
	min	−2·98	−2·19	−1·20	0·26	1·74

ELASTIC SOLUTION $\sigma_{xx}/P=2{\cdot}98$

Table 2. Maximum and minimum values of σ_{yy}/P in element. B—Finite element solution of plate with hole

λ		-1	$-\frac{1}{2}$	0	$\frac{1}{2}$	1
$n=3$	min	−0·93	−1·26	−1·33	−1·30	−1·34
	max.	0·93	0·24	−0·33	−0·80	−1·34
$n=5$	min	−0·93	−1·24	−1·38	−1·36	−1·38
	max	0·92	0·26	−0·38	−0·86	−1·38

theoretical value at the point of symmetry of $\sigma_{xx}/P = 3.00$ compared with a computed value of 2.98.

In Table 2 the maximum and minimum stress at point B are given. The maximum values remains relatively insensitive to the value of n and λ, and clearly no drastic effects occur due to variable load.

Therefore we see that the behaviour of a stress concentration for a creeping body subject to variable proportional loading is very similar to that shown in the two bar structure. Either the maximum stress remains close to the steady state value corresponding to the maximum load, or the stress oscillates between near equal positive and negative values with an amplitude given by the elastic solution.

When variable temperature occurs the situation is of course more complex and this question, for stress concentrations is discussed in [11].

Acknowledgements—The work in this paper was supported by a grant from the Science Research Council, whose assistance is gratefully acknowledged. The calculations were carried out with the assistance of Phillip Brown and his help is gratefully acknowledged.

REFERENCES

1. A. R. S. Ponter, On the stress analysis of creeping structures subject to variable loading. *Trans. ASME, J. Appl. Mech.* **40**, 589 (1973).
2. C. R. Calladine, Time-scales for redistribution of stress in the creep of structures. *Proc. Roy. Soc., London, Series A* **309**, 363 (1969).
3. I. M. Bill and A. C. MacKenzie, Reference stress for redistribution time in creep of structures. *J. Mech. Engng Sci.* **11**(4), 429 (1969).
4. J. J. Williams and F. A. Leckie, A method for estimating creep deformation of structures subject to cyclic loading. *Trans. ASME, J. Appl. Mech.* **40**, 928 (1973).
5. A. R. S. Ponter and J. J. Williams, Work bounds and associated deformation of structures subject to cyclic loading. *Trans. ASME, J. Appl. Mech.* **40**, 921 (1973).
6. A. R. S. Ponter and F. A. Leckie, Bounding solutions for a plate subjected to variable surface temperature. *Trans. ASME, J. Appl. Mech.* **41**, 941 (1974).
7. A. R. S. Ponter, The optimality condition for an upper bound on the displacement of a creeping body subjected to variable loading. *Int. J. Solids Structures* **11**, 1203 (1975).
8. J. H. Lambermont and J. F. Besselling, An experimental and theoretical investigation of creep under uniaxial stress of an Mg-alloy. *IUTAM Symposium on Creep of Structures*, Gothenburg, 17–21 Aug., 1970.
9. A. R. S. Ponter and F. A. Leckie, Constitutive relationships for the time-dependent deformation of metals. *Trans. ASME, Journal of Engineering Materials and Technology*, Paper No. 75-Mat.-3, 1975.
10. A. R. S. Ponter, Deformation bounds for the Bailey–Orowan theory of creep. *Trans. ASME. J. Appl. Mech.* To be published.
11. A. R. S. Ponter and P. Brown, The finite element solution of rapid cycling creep problems. *Report No.* 75-20. Department of Engineering, University of Leicester.